TELKOMNIKA Telecommunication, Computing, Electronics and Control
Vol. 19, No. 1, February 2021, pp. 27∼35
ISSN: 1693-6930, accredited First Grade by Kemenristekdikti, No: 21/E/KPT/2018
DOI: 10.12928/TELKOMNIKA.v19i1.16138

Investigation on energy harvesting enabled device-to-device networks in presence of co-channel interference

Thanh-Luan Nguyen[1], **Dinh-Thuan Do**[2]
[1]Faculty of Electronics Technology, Industrial University of Ho Chi Minh City (IUH), Ho Chi Minh City, Vietnam
[2]Wireless Communications Research Group, Faculty of Electrical and Electronics Engineering, Ton Duc Thang University, Ho Chi Minh City, Vietnam

Article Info

Article history:

Received Mar 25, 2020
Revised Jul 7, 2020
Accepted Sep 24, 2020

Keywords:

Amplify-and-forward
Co-channel interference
Energy harvesting
Ergodic capacity
Outage capacity

ABSTRACT

Energy harvesting from ambient radio-frequency (RF) sources has been a novel approach for extending the lifetime of wireless networks. In this paper, a cooperative device-to-device (D2D) system with the aid of energy-constrained relay is considered. The relays are assumed to be able to harvest energy from information signal and co-channel interference (CCI) signals broadcasted by nearby traditional cellular users and forward the source's signal to its desired destination (D2D user) utilizing amplify-and-forward (AF) relaying protocol. Time switching protocol (TSR) and power splitting protocol (PSR) are proposed to assist energy harvesting and information processing at the relay. The proposed approaches are applied in a model with three nodes including the source (D2D user), the relay and the destination (D2D user), the system throughput is investigated in terms of the ergodic capacity and the outage capacity, where the analytical results are obtained approximately. Our numerical results verify the our derivations, and also points out the impact of CCI on system performance. Finally, this investigation provide fundamental design guidelines for selecting hardware of energy harvesting circuits that satisfies the requirements of a practical cooperative D2D system.

This is an open access article under the CC BY-SA license.

Corresponding Author:

Dinh-Thuan Do
Wireless Communications Research Group
Faculty of Electrical and Electronics Engineering
Ton Duc Thang University, Ho Chi Minh City, Vietnam
Email: dodinhthuan@tdtu.edu.vn

1. INTRODUCTION

Recent advances in energy harvesting technology has indicated that far-field wireless power transfer can also provide interesting aspects in wireless communication systems [1–7]. Notice that the source signals carry both energy and information at the same time. Hence, a hypothesis receiver which can process the information and harvest energy simultaneously is required [8, 9]. However, such device is difficult to implement since the limitation of circuitry. Furthermore, harvesting protocols for information processing and energy harvesting separately have been mentioned in many scientific papers [10, 11]. In cooperative device-to-device (D2D) networks, an intermediate relay is deployed between D2D users to enhance the coverage rate and throughput of communication systems [12, 13].

For both time-switching relaying (TSR) and power-splitting relaying (PSR) protocols, the co-channel interference (CCI) signals act as unnecessary signals, i.e. noises, in information processing phase; on the contrary, supply energy for forwarding information signal in the energy harvesting phase. More importantly, energy harvesting (EH) can be implemented in modern networks such as device-to-device (D2D) networks, small cell networks as many recent works in [14–18]. The authors in [14] examined joint optimization problem to maximize the energy efficiency evaluation related to D2D pairs together with the amount of harvested power by cellular user equipment. We need more complex technologies for D2D communications in some way in cellular bands [15–18]. The impacts of CCI signals are also considered in [19–24]. Motivated by these recent works, we continue to fill gap in the system performance under considering energy harvesting protocols in D2D scenario under impact of CCI by traditional cellular users. In this paper, the TSR and PSR receiver architectures and the corresponding protocols are also adopted. A three-node model of amplify-and-forward (AF) relaying is proposed for both protocols, where the source node can only communicate with destination node with the aid of an intermediate energy-constrained relay node.

2. SYSTEM MODEL

Figure 1 illustrates the system model for the underlay D2D in which two devices, namely UED_S and UED_D, participate in the communication through a controlling base station (BS). Assuming heavily blocked line-of-sight (LOS) path from UED_S to UED_D, the EH-D2D relay is then deployed to assist the transmission. In addition, the relay harvests energy from the RF-signal emitted from the UED_S and each interferer UEC_i, $i = 1, ..., M$. Both the source-to-relay link and relay-to-destination link transmission experience quasi-static independent flat Rayleigh fading with the average gain $\mathbb{E}\{|h_S|^2\} = \Omega_S$ and $\mathbb{E}\{|h_D|^2\} = \Omega_D$, respectively, in which $\mathbb{E}\{\cdot\}$ specifies expectation operator. It is previously stated that the CUEs are the cross-mode interferers and can be treated as CCIs at the relay in the proposed model. The CCIs deteriorate the system performance but surprisingly aid the energy harvesting process at the relay.

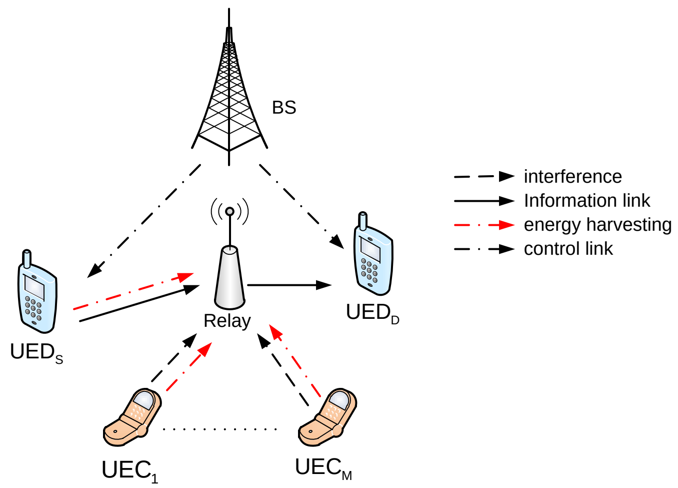

Figure 1. System model of D2D network under impact of the co-channel interferences

3. TIME SWITCHING-BASED RELAYING PROTOCOL

Complying with the TSR-assisted relay architecture, after receiving the RF-signal broadcasted by UED_S, the relay passes the signal to the energy harvesting receiver for a duration of $\xi_r T$ block time and then to the information receiver for that of $(1 - \xi_r) T/2$ block time [12]. Accordingly, the relay performs energy harvesting process and then information process, respectively. Under the presences of the UECs, i.e., the cellular users, the received signal at node R is modeled as

$$y_R(t) = h_S s(t) + \sum_{i=1}^{M} l_i s_i(t)(t) + \tilde{n}_{R[a]}(t), \tag{1}$$

where $s(t)$ is the information signal with power of $\mathcal{P}_S \triangleq \mathbb{E}\{|s(t)|^2\}$, $h_S \in \mathbb{C}$ is the complex channel factor from UED_S to R, $s_i(t)$ specifies the i-th interference signal with the power of $\mathcal{P}_i \triangleq \mathbb{E}\{|s_i(t)|^2\}$, $l_i \in \mathbb{C}$

denotes complex channel factor from UEC_i to R, the number of CCIs is denoted by M and $\tilde{n}_{R[a]}(t)$ is the corrupted narrow band Gaussian noise observed at the receiving antenna. Subsequently, the received signal is converted to a basebanded complex signal after the down conversion process, which results the sampled baseband signal $y_R(k)$ given by

$$y_R(k) = h_S s(k) + \sum_{i=1}^{M} l_i s_i(k) + \underbrace{n_{R[a]}(k) + n_{R[c]}(k)}_{\triangleq n_R^{\mathrm{TSR}}(k)}, \quad (2)$$

where $s_i(k)$ and $s(k)$ denote the signals induced after sampling the i^{th} interfererence signal and the source signal, respectively, $n_{R[a]}(k)$ is the baseband additive white Gaussian noise (AWGN) at the receiving antenna, and $n_{R[c]}(k)$ is the sampled AWGN induced after being converted to baseband, $s_i(k)$ and $s(k)$ have zero means and variance of $N_{R[a]}$ and $N_{R[c]}$, respectively, and $n_R^{\mathrm{TSR}}(k)$ is defined as the total Gaussian noise at node R introduced from adopting the TSR architecture.

The relay then utilizes $\xi_r T$ block time to harvest energy from the received signals. Hence, the energy harvested at the relay is given by

$$E_h = \xi_e \left(\mathcal{P}_S |h_S|^2 + \sum_{i=1}^{M} \mathcal{P}_i |l_i|^2\right) \xi_r T, \quad (3)$$

where ξ_e, with $0 \leq \xi_e \leq 1$ represents the efficiency of the energy harvester, its value depends on the manufacturer. Assuming that the relay fully absorbs the harvested energy to forward the received signal to the other D2D user, i.e., the $\mathrm{UED_D}$ node. Accordingly, the transmit power at the relay can be obtained as

$$\mathcal{P}_R = \frac{E_h}{(1-\xi_r)T/2} = \frac{2\xi_r \xi_e}{1-\xi_r} \left(\mathcal{P}_S |h_S|^2 + \sum_{i=1}^{M} \mathcal{P}_i |l_i|^2\right), \quad (4)$$

As a priority, the relay amplifies the received signal with a gain factor G and then forwards $y_R(k)$ to $\mathrm{UED_D}$. The gain factor G is given by

$$G = \frac{\sqrt{\mathcal{P}_R}}{\sqrt{\mathcal{P}_S |h_S|^2 + \sum_{i=1}^{M} \mathcal{P}_i |l_i|^2 + N_R^{\mathrm{TSR}}}}, \quad (5)$$

where $N_R^{\mathrm{TSR}} \triangleq N_{R[a]} + N_{R[c]}$ denotes the total Gaussian noise power observed at the relay under TSR protocol. Secondly, the received signal at $\mathrm{UED_D}$ after being sampled, $y_D(k)$ is given by

$$y_D(k) = h_S s(k) h_D G + \left(\sum_{i=1}^{M} l_i s_i(k) + n_R^{\mathrm{TSR}}(k)\right) h_D G + n_D(k). \quad (6)$$

4. POWER SPLITTING-BASED RELAYING PROTOCOL

Let P be the received power at R and β, $0 \leq \beta \leq 1$, denote the energy harvesting ratio of the PSR protocol, thus βP specifies the amount of power inputted into the energy harvester. The remaining power, i.e., $(1-\beta)P$, inputs the information transmission to forward the $\mathrm{UED_S}$'s signal to $\mathrm{UED_D}$. Under the presences of cross-mode CCIs, the received signal observed at the relay antenna is

$$y_R(t) = h_S s(t) + \sum_{i=1}^{M} l_i s_i(t)(t) + \tilde{n}_{R[a]}(t). \quad (7)$$

The sampled baseband signal at the relay node, $y_R(k)$, is given by

$$y_R(k) = \sqrt{(1-\beta)} h_S s(k) + \sqrt{1-\beta} \sum_{i=1}^{M} l_i s_i(k) + \underbrace{\sqrt{1-\beta} n_{R[a]}(k) + n_{R[c]}(k)}_{\triangleq n_R^{\mathrm{PSR}}(k)}, \quad (8)$$

in which $n_R^{\mathrm{PSR}}(k)$ denotes the total Gaussian noise introduced by the PSR-assisted relay.

At the relay, an amount of received signal, is adopted for energy harvesting. Hence, the energy harvested at the node R is

$$E_h = \xi_e \left(\mathcal{P}_S |h_S|^2 + \sum_{i=1}^{M} \mathcal{P}_i |l_i|^2\right) \xi_r T. \quad (9)$$

Assume that the harvested energy is perfectly consumed by the relay. As a result, the transmit power at the node R is expressed as

$$\mathcal{P}_R = \frac{E_H}{T/2} = \xi_e \left(\mathcal{P}_S \left| h_S \right|^2 + \sum_{i=1}^{M} \mathcal{P}_i \left| l_i \right|^2 \right) \beta. \tag{10}$$

Similarly, the relay firstly amplifies the received signal with the gain factor, G, which can be expressed as

$$G = \frac{\sqrt{\mathcal{P}_R}}{\sqrt{\left(1-\beta\right) \mathcal{P}_S \left| h_S \right|^2 + \left(1-\beta\right) \sum_{i=1}^{M} \mathcal{P}_i \left| l_i \right|^2 + N_R^{\mathrm{PSR}}}}, \tag{11}$$

where $N_R^{\mathrm{PSR}} \triangleq \left(1-\beta\right) N_{R[a]} + N_{R[c]}$. Accordingly, the received signal after the being sampled at the destination node, $y_D\left(k\right)$, is given by

$$y_D(k) = h_S s(k) h_D G + \left(\sum_{i=1}^{M} l_i s_i(k) + n_R^{\mathrm{PSR}}(k) \right) h_D G + n_D(k). \tag{12}$$

5. GENERAL ANALYSIS

We find that the TSR and PSR protocols have similar mechanisms, deriving a general form for the signal-to-noise-plus-interence ratio (SINR) can be feasible. In order to derive an unified result, we define $n_R^{\mathrm{Y}}\left(k\right)$ as the total Gaussian noise at the relay with variance of $N_R^{\mathrm{Y}}\left(k\right)$ for the $\mathrm{Y} \in \{\mathrm{TSR}, \mathrm{PSR}\}$ protocol, the expressions of $n_R^{\mathrm{TSR}}\left(k\right)$ and $n_R^{\mathrm{PSR}}\left(k\right)$ are defined in the previous section. Therefore, the unified form of the achievable end-to-end SINR under the adoption of the protocol Y, denoted by Ψ_{gen}^{Y}, can be expressed as

$$\Psi_{gen}^{\mathrm{Y}} = \frac{\gamma_1}{\gamma_{INF} + \frac{1}{\gamma_g^{\mathrm{Y}}} \left(1 + \frac{N_R^{\mathrm{Y}}}{\gamma_1 + \gamma_{INF}} \right) + N_R^{\mathrm{Y}}}, \tag{13}$$

in which $\gamma_1 \triangleq \mathcal{P}_S |h_S|^2$, $\gamma_{INF} \triangleq \sum_{i=1}^{M} \mathcal{P}_i |l_i|^2$, $\gamma_g^{\mathrm{TSR}} \triangleq \frac{2\xi_r \xi_e}{1-\xi_r} \frac{|h_D|^2}{N_D}$ and $\gamma_g^{\mathrm{PSR}} \triangleq \beta \xi_e \frac{|h_D|^2}{N_D}$. Hereafter, we define $\mathrm{SNR} \triangleq \mathcal{P}_S \Omega_S / N_D$ as the average signal-to-noise ratio (SNR).

5.1. Outage probability

In this paper, considering the whole system, an outage event occurs whenever Ψ_{gen}^{Y} drops below an acceptable threshold, γ_{th} (dB). Accordingly, the outage probability is defined as

$$P_{out}^{\mathrm{Y}} = \Pr\left(\Psi_{gen}^{\mathrm{Y}} < \gamma_{th} \right) = F_{\Psi_{gen}^{\mathrm{Y}}}\left(\gamma_{th} \right). \tag{14}$$

It is not tractable to derive the exact outage probability in closed-form from (14). Hence, to simplify the calculation, we apply the high SNR approximation. At high SNR, where the $\mathrm{UED_S}$ transmits with relatively high power level, the term "$\mathrm{N}_R^{\mathrm{Y}}/(\gamma_1 + \gamma_{INF})$" in the denominator of (13) can be negligible. As a result, the approximated SINR at the relay is given by

$$\Psi_{gen}^{\mathrm{Y}} \approx \frac{\gamma_1}{\gamma_{INF} + \frac{1}{\gamma_g^{\mathrm{Y}}} + \mathrm{N}_R^{\mathrm{Y}}}. \tag{15}$$

Therefore, the approximated outage probability, P_{out}^{Y}, in (14) is then rewritten as

$$F_{\Psi_{gen}^{\mathrm{Y}}}(\gamma_{th}) \approx \int_0^\infty \int_0^\infty \Pr\left(\gamma_1 < \gamma_{th} \left(z + \frac{1}{y} + N_R^{\mathrm{Y}} \right) \right) f_{\gamma_{INF}}(y) f_{\gamma_g^{\mathrm{Y}}}(z) dy dz. \tag{16}$$

Note that γ_g^{TSR} and γ_g^{PSR} are random variables having exponential distribution. Subsequently, the probability density function (PDF) of γ_g^{Y} is given by

$$f_{\gamma_g^{\mathrm{Y}}}\left(z\right) \triangleq \frac{1}{\bar{\gamma}_g^{\mathrm{Y}}} \exp\left\{ -\frac{z}{\bar{\gamma}_g^{\mathrm{Y}}} \right\}, \; z > 0, \tag{17}$$

where $\bar{\gamma}_g^{\mathrm{TSR}} \triangleq \frac{2\xi_r\xi_e}{1-\xi_r}\frac{\Omega_D}{N_D}$ and $\bar{\gamma}_g^{\mathrm{PSR}} = \xi_e\beta\frac{\Omega_D}{N_D}$. In addition, the CDF of γ_1 is $F_{\gamma_1}(x) = 1 - \exp\left\{-\frac{x}{\bar{\gamma}_1}\right\}$, where $\bar{\gamma}_1 \triangleq \mathcal{P}_S\Omega_S$ and the PDF of γ_{INF} is given by

$$f_{\gamma_{INF}}(y) = \sum_{i=1}^{v(\boldsymbol{\mathcal{D}})}\sum_{j=1}^{\tau_i(\boldsymbol{\mathcal{D}})} \chi_{i,j}(\boldsymbol{\mathcal{D}})\frac{\mu_{\langle i\rangle}^{-j}}{(j-1)!}y^{j-1}\exp\left\{-\frac{y}{\mu_{\langle i\rangle}}\right\},\ y > 0, \tag{18}$$

in which $\boldsymbol{\mathcal{D}} = \mathrm{diag}\left(\mu_1, \mu_2, ..., \mu_M\right)$ specifies a diagonal matrix with the eigenvalues of $\mu_i = \frac{\mathcal{P}_i}{N_D}\Omega_i$, $v\left(\boldsymbol{\mathcal{D}}\right)$ denotes the number of distinct diagonal elements, $\mu_{\langle 1\rangle} > \mu_{\langle 2\rangle} > ... > \mu_{\langle v(\boldsymbol{\mathcal{D}})\rangle}$ are the distinct diagonal elements in descending order, $\tau_i\left(\boldsymbol{\mathcal{D}}\right)$ is the multiplicity of $\mu_{\langle i\rangle}$, and $\chi_{i,j}(\boldsymbol{\mathcal{D}})$ is the (i,j)-th characteristic coefficient of the matrix $\boldsymbol{\mathcal{D}}$ [24]. Substituting (18) and (17) into (16), the approximated P_{out}^{Y} expressed in the integral-form is given by

$$\begin{aligned}P_{out}^{\mathrm{Y}} \approx& 1 - \frac{1}{\bar{\gamma}_g^{\mathrm{Y}}}\exp\left\{-\frac{N_R^{\mathrm{Y}}\gamma_{th}}{\bar{\gamma}_1}\right\}\sum_{i=1}^{v(\boldsymbol{\mathcal{D}})}\sum_{j=1}^{\tau_i(\boldsymbol{\mathcal{D}})}\frac{\chi_{i,j}(\boldsymbol{\mathcal{D}})}{(j-1)!}\\ &\times\frac{1}{\mu_{\langle i\rangle}^{j}}\underbrace{\int_0^\infty y^{j-1}\exp\left\{-\left(\frac{\gamma_{th}}{\bar{\gamma}_1}+\frac{1}{\mu_{\langle i\rangle}}\right)\right\}dy}_{I_1}\underbrace{\int_0^\infty \exp\left\{-\frac{\gamma_{th}}{\bar{\gamma}_1}-\frac{z}{\bar{\gamma}_g^{\mathrm{Y}}}\right\}dz}_{I_2}.\end{aligned} \tag{19}$$

Subsequently, the above integrals (I_1 and I_2) can be derived in closed-form with the help of [25, (2.3.3.1)] and [25, (2.3.16.1)] as

$$I_1 = \int_0^\infty y^{j-1}\exp\left\{-\left(\frac{\gamma_{th}}{\bar{\gamma}_1}+\frac{1}{\mu_{\langle i\rangle}}\right)y\right\}dy = \Gamma(j)\left(\frac{\gamma_{th}}{\bar{\gamma}_1}+\frac{1}{\mu_{\langle i\rangle}}\right)^{-j}, \tag{20}$$

$$I_2 = \int_0^\infty \exp\left\{-\frac{\gamma_{th}}{\bar{\gamma}_1 z}-\frac{z}{\bar{\gamma}_g^{\mathrm{Y}}}\right\}dz = 2\left(\frac{\gamma_{th}\bar{\gamma}_g^{\mathrm{Y}}}{\bar{\gamma}_1}\right)^{1/2}K_1\left(2\sqrt{\frac{\gamma_{th}}{\bar{\gamma}_1\bar{\gamma}_g^{\mathrm{Y}}}}\right), \tag{21}$$

respectively, where $K_v\left(\cdot\right)$ denotes the v-th order modified Bessel function of the second kind and $\Gamma(x)$ specifies the Gamma function. Hence, the outage probability P_{out}^{Y} can be approximated by using (21), (20) and (19) which then results the following equation after some algebraic steps

$$P_{out}^{\mathrm{Y}} \approx 1 - \sqrt{\frac{4\gamma_{th}}{\bar{\gamma}_g^{\mathrm{Y}}\bar{\gamma}_1}}K_1\left(\sqrt{\frac{4\gamma_{th}}{\bar{\gamma}_g^{\mathrm{Y}}\bar{\gamma}_1}}\right)\exp\left\{-\frac{N_R^{\mathrm{Y}}\gamma_{th}}{\bar{\gamma}_1}\right\}\sum_{i=1}^{v(\boldsymbol{\mathcal{D}})}\sum_{j=1}^{\tau_i(\boldsymbol{\mathcal{D}})}\chi_{i,j}(\boldsymbol{\mathcal{D}})\left(1+\frac{\mu_{\langle i\rangle}\gamma_{th}}{\bar{\gamma}_1}\right)^{-j}. \tag{22}$$

When the interfering signals are statistically independent and identically distributed (i.i.d.), i.e., $\mu_i = \mu, i = 1, 2, ..., M$, then $v\left(\boldsymbol{\mathcal{D}}\right) = 1$ and $\tau_i\left(\boldsymbol{\mathcal{D}}\right) = M$, the outage probability, P_{out}^{Y}, is then reduced to

$$P_{out}^{\mathrm{Y}} = 1 - \sqrt{\frac{4\gamma_{th}}{\bar{\gamma}_g^{\mathrm{Y}}\bar{\gamma}_1}}K_1\left(\sqrt{\frac{4\gamma_{th}}{\bar{\gamma}_g^{\mathrm{Y}}\bar{\gamma}_1}}\right)\exp\left\{-\frac{N_R^{\mathrm{Y}}\gamma_{th}}{\bar{\gamma}_1}\right\}\left(1+\frac{\mu\gamma_{th}}{\bar{\gamma}_1}\right)^{-M}. \tag{23}$$

5.2. Outage capacity and achievable throughput

The outage capacity for the AF cooperative D2D system under consideration is given by

$$C_O^{\mathrm{Y}} = \left[1 - P_{out}^{\mathrm{Y}}\right]\log_2\left(1+\gamma_{th}\right) \tag{24}$$

The achievable throughput is defined in terms of effective transmission block time, which is the block time utilized for relay-to-destination transmission. According to [24], the achievable throughput of a cooperative system is given by

$$\tau_O^{\mathrm{Y}} = \begin{cases}\dfrac{(1-\xi_r)T/2}{T}C_O^{\mathrm{TSR}} & , \mathrm{Y} \equiv \mathrm{TSR}\\ \dfrac{T/2}{T}C_O^{\mathrm{PSR}} & , \mathrm{Y} \equiv \mathrm{PSR}\end{cases} = \begin{cases}(1-\xi_r)C_O^{\mathrm{TSR}}/2 & , \mathrm{Y} \equiv \mathrm{TSR}\\ C_O^{\mathrm{PSR}}/2 & , \mathrm{Y} \equiv \mathrm{PSR}\end{cases} \tag{25}$$

5.3. Ergodic capacity and achievable throughput

In this subsection, the throughput achieved by evaluating the Ergodic capacity in the unit of bits/Hz is derived as the third important metrics to evaluate the system performance. In the AF-cooperative D2D communication, using Ψ_{gen}^{Y} in (8), the received SINR at the relay, C_E is given by

$$C_E^{\mathrm{Y}} = \mathbb{E}\left\{\frac{1}{2}\log_2(1+\Psi_{gen}^{\mathrm{Y}})\right\} = \int_0^{\infty} \log_2(1+\varpi) f_{\Psi_{gen}^{\mathrm{Y}}}(\varpi)d\varpi, \tag{26}$$

where $f_{\Psi_{gen}^{\mathrm{Y}}}(\varpi)$ stands for the PDF of the random variable Ψ_{gen}^{Y}. Applying the integration by parts for the integral in (32), the above expression becomes

$$\begin{aligned} C_E^{\mathrm{Y}} = & \left[\log_2(1+\varpi)(F_{\Psi_{gen}^{\mathrm{Y}}}(\varpi)-1)\right]\Big|_0^{\infty} \\ & - \frac{1}{\ln 2}\int_0^{\infty} \frac{1}{1+\varpi}[F_{\Psi_{gen}^{\mathrm{Y}}}(\varpi)-1]d\varpi \qquad (27) \\ = & \frac{1}{\ln 2}\int_0^{\infty} \frac{1}{1+\varpi}(1-F_{\Psi_{gen}^{\mathrm{Y}}}(\varpi))d\varpi, \qquad (28) \end{aligned}$$

where $\{f(x)\}_a^b \triangleq f(b) - f(a)$. Similarly as in 5.2, the throughput at the destination depends only on the effective transmission time, $(1-\xi_r)T/2$ for TSR protocol and $T/2$ for PSR protocol, and can be expressed as

$$\tau_E^{\mathrm{Y}} = \begin{cases} (1-\xi_r)C_O^{\mathrm{TSR}}/2 & , \mathrm{Y} \equiv \mathrm{TSR} \\ C_O^{\mathrm{PSR}}/2 & , \mathrm{Y} \equiv \mathrm{PSR} \end{cases} \tag{29}$$

6. NUMERICAL RESULTS

In this section, the simulation results and the approximated analytical results are derived. To evaluate the effects of the interference on the system throughput we define SIR $\triangleq \frac{\mathcal{P}_S \Omega_S}{\sum_{i=1}^{M} \mathcal{P}_i \Omega_i}$ as the average signal-to-interference ratio. The variances are assumed to the identical and kept fixed, that is $N_D = 1$, $N_{R[a]} = N_{R[c]} = 1$ and the SINR threshold, is set to 8 dB unless stated otherwise. In Figures 2-5, we assume a single interferer ($M = 1$). In addition, the energy conversion efficiency is set to 1 ($\xi_e = 1$). Importantly, in order to evaluate the impact of the interference on the throughput, we define $\|\mu\| = \frac{\mu}{\{\gamma_{INF}\}}$ as the normalized power distribution, where $\mu = \left(\mu_{\langle 1\rangle}, \mu_{\langle 2\rangle}, ..., \mu_{\langle M\rangle}\right)$.

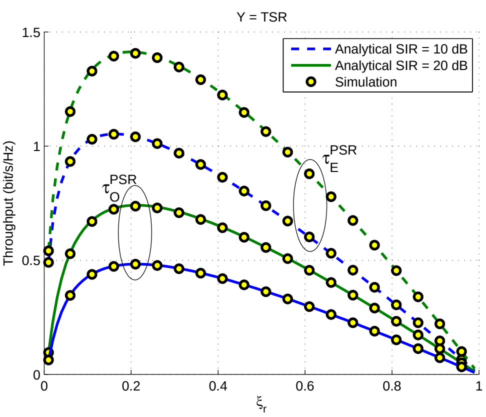

Figure 2. Throughput as a function of the energy harvesting ratio with two values of the average SIR, the average SNR is set to 20 dB

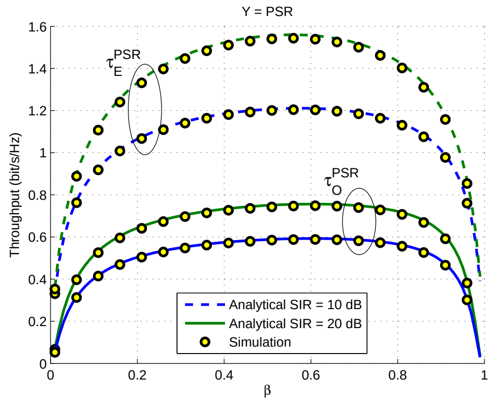

Figure 3. Throughput τ_E^{TSR},τ_O^{TSR}, τ_E^{PSR} and τ_O^{PSR} as a function of the average SNR, in which SIR = 10 dB

Figure 2 shows throughput τ_E^{TSR} and τ_O^{TSR} versus the energy harvesting ratio ξ_r for different values of average SIR where SNR is set to 20 dB. The simulation results of τ_E^{TSR} are evaluated, where C_E^{Y} and Ψ_{gen}^{Y} are obtained. The solid curves are the corresponding approximated analytical results of τ_E^{TSR} which derived in (33). The dashed curves are the corresponding approximated analytical results of τ_O^{TSR} derived. It is observed in Figure 3 that the throughput increases as the energy harvesting ratio, ξ_r increases from 0 to some optimal value but later as ξ_r continues increasing, the relay wastes more time on energy harvesting rather than information transmission resulting that the throughput of the system starts dropping down from its maximum value.

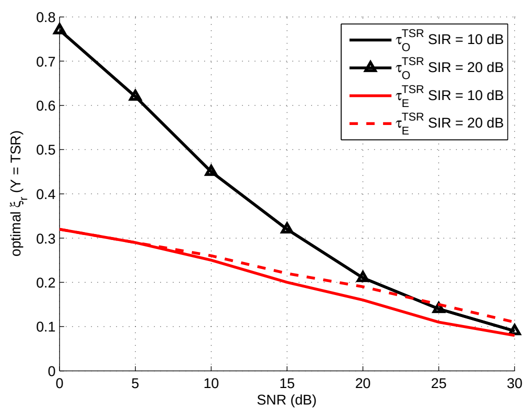

Figure 4. Optimal ξ_r versus the average SNR for different values of the average SIR

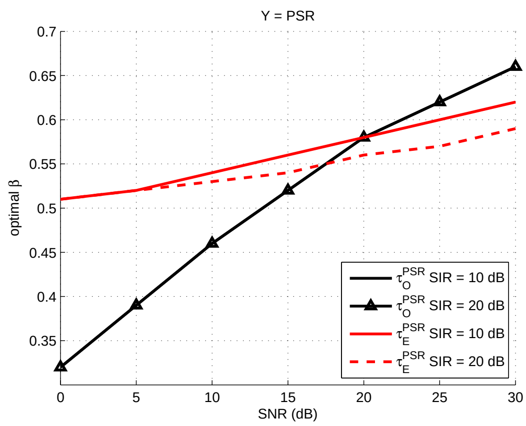

Figure 5. Optimal β versus the average SNR for different values of the average SIR

Figure 4 and Figure 5 shows the optimal ξ_r and optimal β, respectively, the corresponding optimal throughputs where the average SIR is set to 10 dB are illustrated in Figure 3. It is seen that, in TSR protocol, as the average SNR increases the optimal ξ_r decreases. This implies that the system performance can effectively be enhanced and the time spent for energy harvesting ($\xi_r T$) can also be reduced by increasing the transmit power of the source, $\mathcal{P}_S$. In addition, the optimal ratios to achieve the optimal throughput τ_E^{TSR} increases as the average SIR increases. However, the similar trend does not apply to optimal τ_O^{TSR}, in this case, the optimal ξ_r does not change as the average SIR increases. The converse happened in PSR protocol, where the optimal β increases as the average SNR increases. Furthermore, the optimal β to achieve the optimal throughput τ_E^{PSR} decreases as the average SIR increases. This implies that, in PSR protocol, more power is used for energy harvesting as the average SNR increases and less power can be needed if there is an increasing in the power of the interference. The impact of CCI power distribution to the system throughput is illustrated in Figure 6 and Figure 7 for system with TSR and PSR protocol, respectively. The energy harvesting ratio ξ_r and β are set to 0.2 and 0.8, respectively. Though the power distributions are different, e.g. $\|\mu_1\| = (1.0,\, 0,\, 0,\, 0)\,,\ \|\mu_2\| =$

$(0.5, 0.5, 0, 0, 0)$ and $\|\mu_1\| = (1.0, 0, 0, 0)$, but the total power of interferers remains the same value. It is observed that, the achievable throughput decreases as the normalized power distribution are changed from $\|\mu_1\|$ to $\|\mu_2\|$ and from $\|\mu_2\|$ to $\|\mu_3\|$.

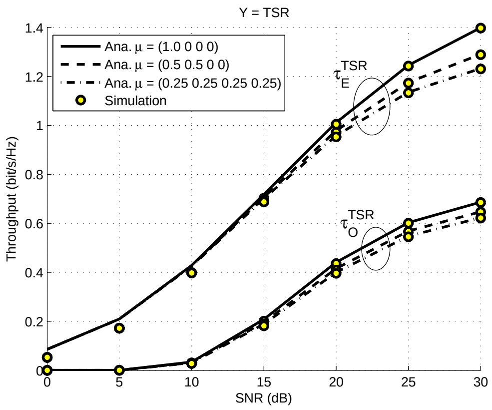

Figure 6. Throughput τ_E^{TSR} and τ_O^{TSR} versus the average SNR under different CCI power distribution where the average SIR is set to 10 dB

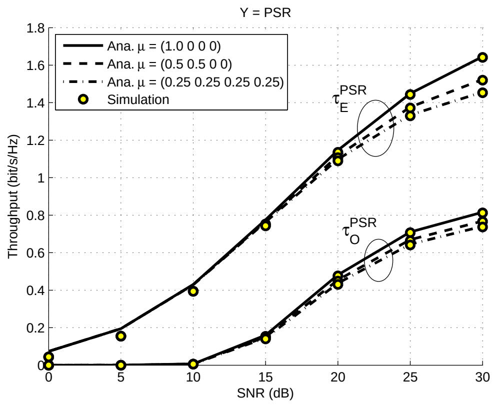

Figure 7. Throughput τ_E^{PSR} and τ_O^{PSR} versus the average SNR under different CCI power distribution where the average SIR is set to 10 dB

7. CONCLUSION

In this paper, an AF cooperative D2D system was proposed where the EH-assisted relay is affected by co-channel interferences (CCI) from the CUEs. The energy-constrained relay absorbs the harvested energy from the received source signal and CCI signals to support the transmission between D2D users. The system performance can be deteriorated if the power of the CCI signals increases. One can effectively increase the system throughput by increasing the average SNR, this can be achieved by increasing the transmit power of D2D users. Lastly, different power distribution can also affect to the system throughput.

REFERENCES

[1] T.-L. Nguyen, D.-T. Do, "Power Allocation Schemes for Wireless Powered NOMA Systems with Imperfect CSI: System model and performance analysis, " *International Journal of Communication Systems*, vol. 31, no. 15, 2018.

[2] D.-T. Do, *et al.*, "Wireless power transfer enabled NOMA relay systems: two SIC modes and performance evaluation," *TELKOMNIKA Telecommunication Computing Electronics and Control*, vol. 17, no.6, pp. 2697-2703, 2019.

[3] D.-T. Do and C. B. Le, "Exploiting Outage Performance of Wireless Powered NOMA," *TELKOMNIKA Telecommunication Computing Electronics and Control*, vol. 16, no. 5, pp. 1907-1917, 2018.

[4] D.-T. Do, M.-S. Van Nguyen, T. A. Hoang, B. M. Lee, " Exploiting Joint Base Station Equipped Multiple Antenna and Full-Duplex D2D Users in Power Domain Division Based Multiple Access Networks," *Sensors*,vol. 19, no. 11, pp. 2475-2494, 2019.

[5] D.-T. Do and C. B. Le, "Application of NOMA in Wireless System with Wireless Power Transfer Scheme: Outage and Ergodic Capacity Performance Analysis," *Sensors*, vol. 18, no. 10, pp. 3501-3517, 2018.

[6] D.-T. Do, M.-S. V. Nguyen, "Outage probability and ergodic capacity analysis of uplink NOMA cellular network with and without interference from D2D pair," *Physical Communication*, vol. 37, 2019.

[7] R. Rajesh, V. Sharma, and P. Viswanath, "Information capacity of energy harvesting sensor nodes," *Proc. 2011 IEEE Int. Symp. Inf. Theory*, pp. 2363-2367, July 2011.

[8] L. R. Varshney, "Transporting information and energy simultaneously," *Proc. 2008 IEEE Int. Symp. Inf. Theory*, pp. 1612-1616, July 2008.

[9] P. Grover, A. Sahai, "Shannon meets Tesla: Wireless information and power transfer," *Proc. 2010 IEEE Int. Symp. Inf. Theory*, pp. 2363-2367, July 2010.

[10] R. Zhang and C. K. Ho, "MIMO broadcasting for simultaneous wireless information and power transfer," *IEEE Trans. Wirel. Commun.*, vol. 12, no. 5, pp. 1989-2001, May 2013.

[11] B. Medepally and N. B. Mehta, "Voluntary energy harvesting relays and selection in cooperative wireless networks," *IEEE Trans. Wirel. Commun.*, vol. 9, no. 11, pp. 3543-3553, November 2010.

[12] A. A. Nasir, X. Zhou, S. Durrani, and R. A. Kennedy, "Relaying protocols for wireless energy harvesting and information processing," *IEEE Trans. Wirel. Commun.*, vol. 7, no. 12, pp. 3622-3636, Nov. 2013.

[13] D. Yang, ”Wireless Information and Power Transfer: Optimal power control in one-way and two-way relay system,” *Wireless Personal Commun.*, vol. 84, no. 1, pp. 1-14, June 2015.

[14] Z. Zhou, C. Gao, C. Xu, T. Chen, D. Zhang and S. Mumtaz, ”Energy-Efficient Stable Matching for Resource Allocation in Energy Harvesting-Based Device-to-Device Communications,” *IEEE Access*, vol. 5, pp. 15184-15196, May 2017.

[15] S. Lee, R. Zhang, and K. Huang, ”Opportunistic wireless energy harvesting in cognitive radio networks,” *IEEE Trans. Wireless Commun.*, vol. 12, no. 9, pp. 4788-4799, September 2013.

[16] S. Gupta, R. Zhang and L. Hanzo, ”Energy Harvesting Aided Device-to-Device Communication Underlaying the Cellular Downlink,” *IEEE Access*, vol. 5, pp. 7405-7413, 2017.

[17] L. Jiang *et al.*, ”Social-aware energy harvesting device-to-device communications in 5G networks,” *IEEE Wirel. Commun.*, vol. 23, no. 4, pp. 20-27, 2016.

[18] M. L. Ku, J. W. Lai, ”Joint Beamforming and Resource Allocation for Wireless-Powered Device-to-Device Communications in Cellular Networks,” *IEEE Trans. Wirel. Commun.*, vol. 16, no. 11, pp. 7290-7304, 2017.

[19] D. W. K. Ng, R. Schober, Spectral efficient optimization in OFDM systems with wireless information and power transfer, *Proc. 21st Eur. Signal Process. Conf.*, pp. 1-5, September 2013.

[20] G. Yang, C. K. Ho, and Y. L. Guan, Dynamic resource allocation for multiple-antenna wireless power transfer, *IEEE Trans. Signal Process.*, vol. 62, no. 14, pp. 3565-3577, Jul. 2014

[21] D.-T. Do, H. S. Nguyen, ”A Tractable Approach to Analyze the Energy-Aware Two-way Relaying Networks in Presence of Co-channel Interference,” *EURASIP Journal on Wireless Communications and Networking*, vol. 2016, no. 271, 2016.

[22] T.-L. Nguyen, D.-T. Do, ”A new look at AF two-way relaying networks: energy harvesting architecture and impact of co-channel interference”, *Annals of Telecommunications*, vol. 72, no. 11, pp. 669-678, 2017.

[23] J. A. Hussein, S. Boussakta and S. S. Ikki, ”Performance Study of a UCRN Over Nakagami- m Fading Channels in the Presence of CCI,” *IEEE Trans. on Cognitive Communications and Networking*, vol. 3, no. 4, pp. 752-765, December 2017.

[24] Y. Gu and S. Aissa, ”Interference aided energy harvesting in decode-and forward relaying systems,” in Proc. *IEEE Int. Conf. Commun.*, pp. 5378-5382, Jun. 2014.

[25] A. P. Prudnikov, Y. A. Brychkov, and O. I. Marichev, Integrals and Series, vols. 1-2. New York, *Gordon and Breach Science Publishers*, 1986.